JOURNAL OF VIROLOGY, Nov. 1995, p. 7362–7366 Vol. 69, No. 11
0022-538X/95/$04.00+0

Herpes Simplex Virus Capsids Assembled in Insect Cells Infected with Recombinant Baculoviruses: Structural Authenticity and Localization of VP26

BENES L. TRUS,[1,2] FRED L. HOMA,[3] FRANK P. BOOY,[1] WILLIAM W. NEWCOMB,[4] DARRELL R. THOMSEN,[3] NAIQIAN CHENG,[1] JAY C. BROWN,[4] AND ALASDAIR C. STEVEN[1]*

Laboratory of Structural Biology, National Institute of Arthritis and Musculoskeletal and Skin Diseases,[1] and Computational Bioscience and Engineering Laboratory, Division of Computer Research and Technology,[2] National Institutes of Health, Bethesda, Maryland 20892-2755; Molecular Biology Research, The Upjohn Company, Kalamazoo, Michigan 49001[3]; and Department of Microbiology and Cancer Center, University of Virginia Health Sciences Center, Charlottesville, Virginia 22908[4]

Received 19 June 1995/Accepted 17 August 1995

Recently, recombinant baculoviruses have been used to show that expression of six herpes simplex virus type 1 genes results in the formation of capsid-like particles. We have applied cryoelectron microscopy and three-dimensional image reconstruction to establish their structural authenticity to a resolution of ~2.7 nm. By comparing capsids assembled with and without the expression of gene UL35, we have confirmed the presence of six copies of its product, VP26 (12 kDa), around each hexon tip. However, VP26 is not present on pentons, indicating that the conformational differences between the hexon and penton states of the major capsid protein, VP5, extend to the VP26 binding site.

The herpes simplex virus type 1 (HSV-1) capsid is one of the largest and most elaborate virus particles, and an understanding of its structure and assembly at the molecular level is beginning to emerge. Its assembly involves the copolymerization of six major proteins—four shell proteins and two internal proteins—and potentially the participation of host factors as well (for a review, see references 19 and 22). In recent years, the capsid structure has been described in progressively greater detail in three-dimensional density maps reconstructed from cryoelectron micrographs (2, 4, 7, 16, 20, 26, 28). Hexons (n = 150) and pentons (n = 12) are arrayed on a T=16 surface lattice (27). The hexons are hexamers of VP5 (149 kDa) (11, 21), and the pentons are pentamers of VP5 (16). On the outer surface, the sites of local threefold symmetry are occupied by "triplexes," which are heterotrimers of VP23 (35 kDa) and VP19c (50 kDa) (16).

The fourth abundant shell protein, VP26, has been localized to the outer tips of hexons by difference mapping between capsids with and without VP26 (4). Because this study was carried out with pentonless capsids, it was not possible to determine whether VP26 was also present on pentons. On the basis of a difference map calculated between one-fifth of a penton and one-sixth of a hexon from a reconstruction of intact capsids, Zhou et al. (28) have proposed that VP26 is absent from pentons. However, conformational differences between penton VP5 and hexon VP5, as expressed in terms of antigenicity (26), susceptibility to proteolysis (17, 21), and extractability with urea (16), are known to exist, which implies that structural differences between hexon and penton protomers may not be strictly additive.

With the development of recombinant baculoviruses, it is now possible to express defined combinations of HSV capsid genes to probe their roles in assembly (23–25). These studies have shown that three shell proteins, VP5 (gene UL19), VP19 (UL38), and VP23 (UL18), and either scaffold protein VP22a (UL26.5) or the protease-scaffold protein (UL26) are required to produce particles that are capsid-like upon examination by thin sectioning and negative staining electron microscopy. VP26 (UL35) (9, 13) is dispensable for assembly but is incor-

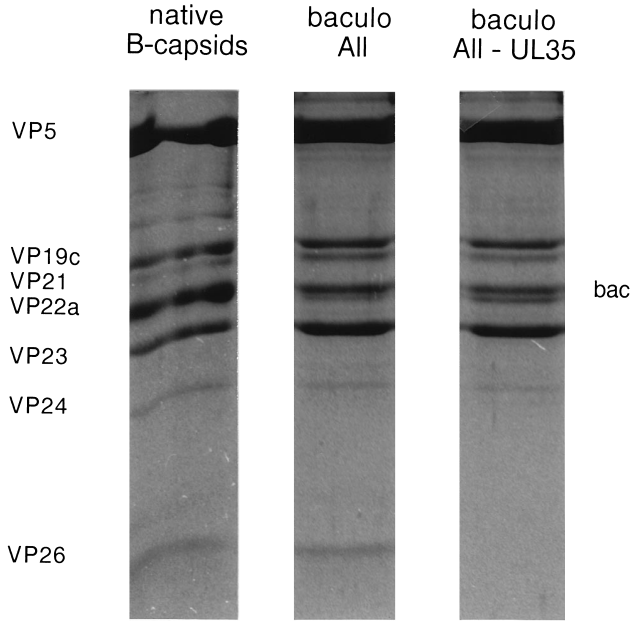

FIG. 1. The protein compositions of HSV-1 capsids purified from recombinant baculovirus expression experiments and that of HSV-1 B capsids isolated from infected BHK cells are compared by sodium dodecyl sulfate-polyacrylamide gel electrophoresis on 13% gels as described previously (14, 16). The separated proteins were detected by staining with Coomassie brilliant blue. All capsids involved the expression of all six genes coding for major capsid proteins, viz., UL19 (VP5), UL38 (VP19c), UL18 (VP23), UL26 (VP21 and VP24), UL26.5 (VP22a), and UL35 (VP26), whereas with All − UL35, the baculovirus expressing UL35 was omitted. Baculovirus-derived HSV-1 capsids tend to have a somewhat lower content of VP22a than native B capsids (25), and small amounts of the baculovirus capsids (bac protein) copurify with them. Otherwise, their protein compositions are essentially indistinguishable, except for the absence of VP26 from All − UL35 capsids.

* Corresponding author. Mailing address: Bldg. 6, Room 425, 6 Center Dr., MSC 2755, National Institutes of Health, Bethesda, MD 20892-2755. Phone: (301) 496-0132. Fax: (301) 402-3417.

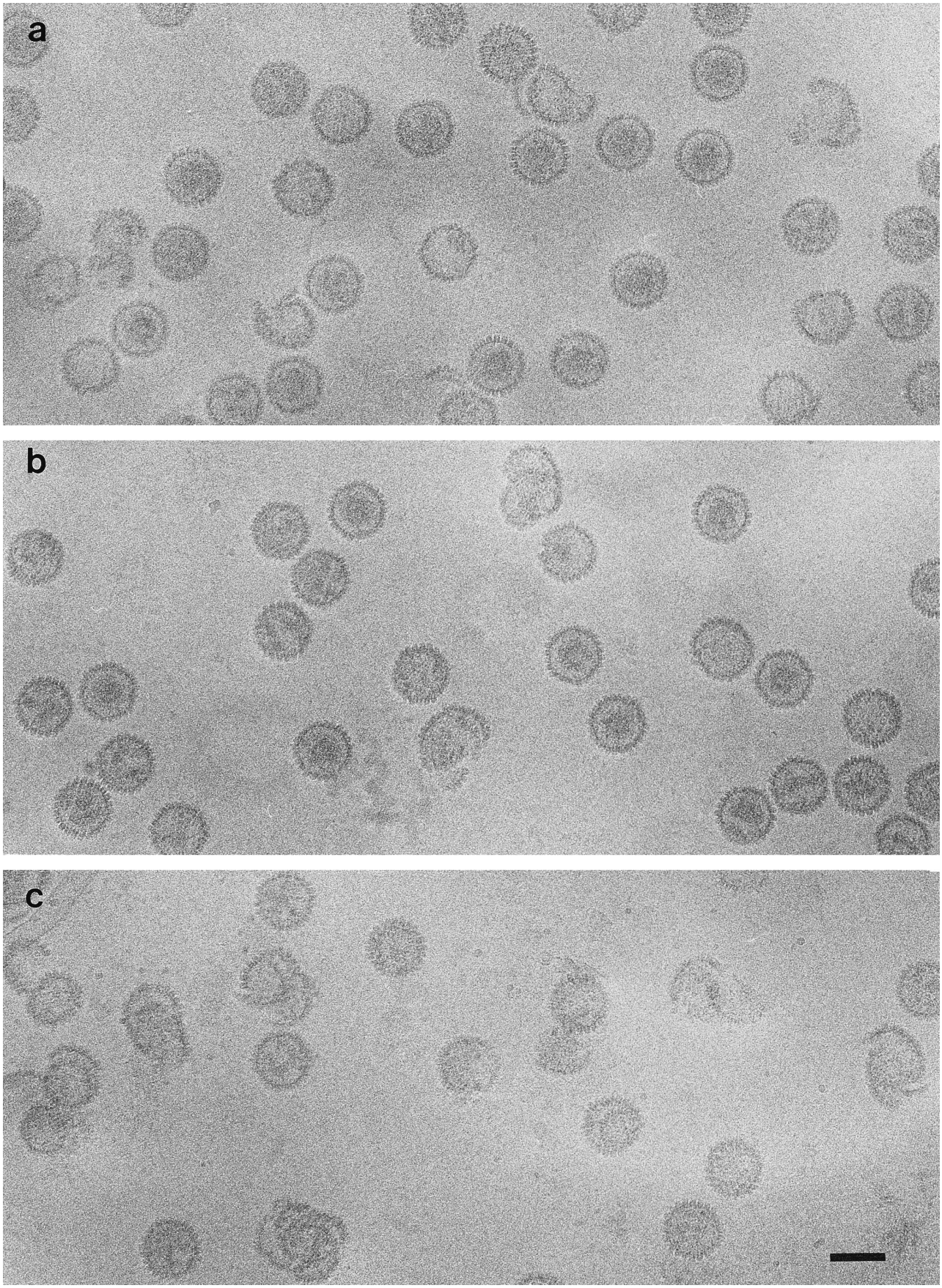

FIG. 2. Cryoelectron micrographs of purified preparations of HSV-1 capsids produced by recombinant baculoviruses expressing HSV-1 genes. (a) All capsids. (b) All − UL35 capsids. (c) All − UL26.5 capsids (the baculovirus expressing UL26.5 was omitted). Bar = 100 nm.

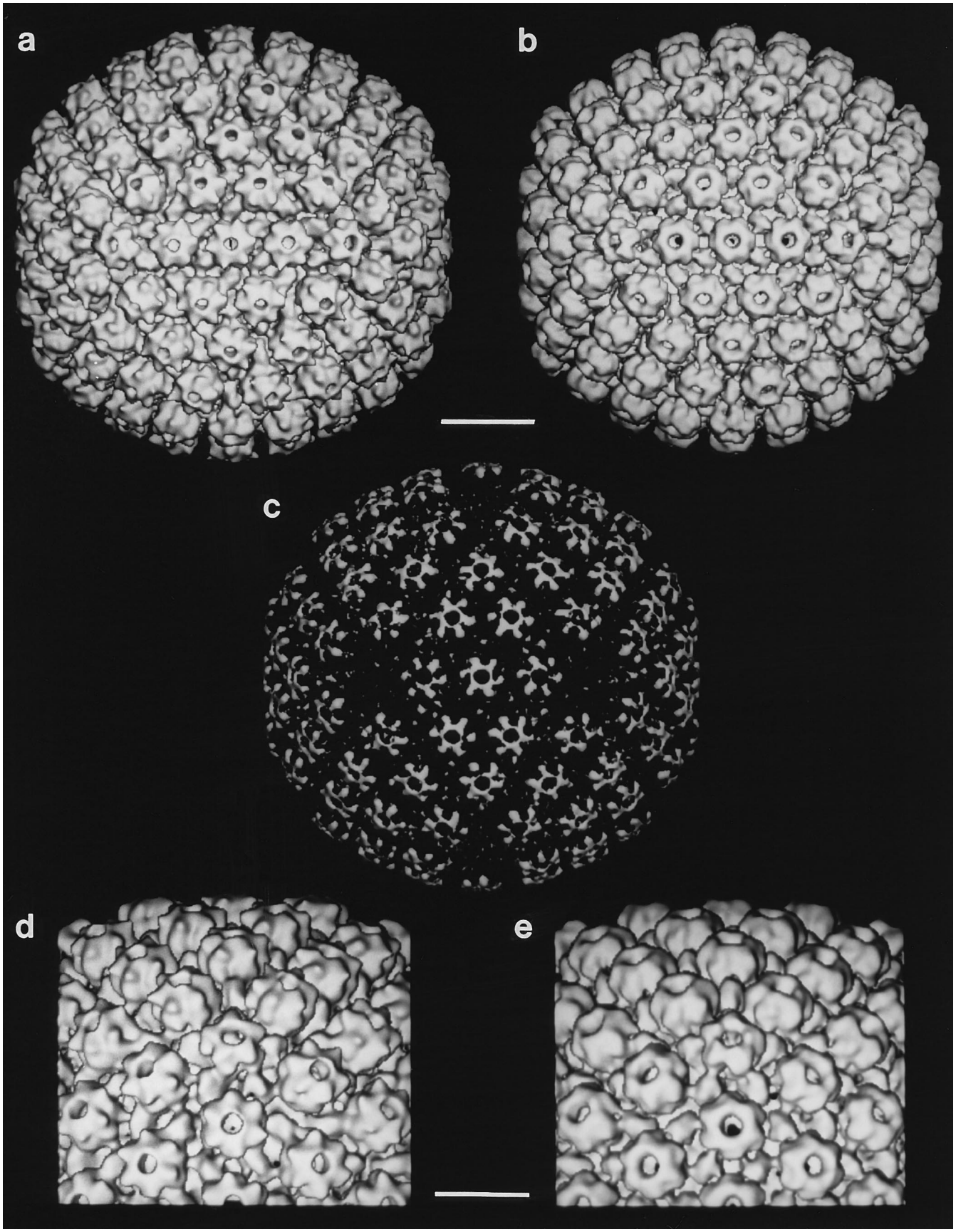
a
b
c
d
e

FIG. 3. Three-dimensional density maps calculated from cryoelectron micrographs of HSV-1 capsids assembled in recombinant baculovirus expression systems. The micrographs analyzed had defocus values for which the first zero of the contrast transfer function was at ~2.5 nm^{-1}. The reconstruction procedure included the use of an Intel iPSC/860 supercomputer to speed computationally intensive tasks (12). The All capsid produced upon coexpression of all six genes coding for major capsid proteins (a and d) and the All − UL35 capsid (b and e) are shown. The outer surfaces of the capsids are viewed along an axis of twofold symmetry (a and b). The difference map calculated between the two reconstructions is shown (c). Bar (a, b, and c) = 50 nm. At higher magnification, the pentons (d) and triplexes (e) are very similar, but six outcrops of density that are present around the outer rim of All hexons are missing from All − UL35 hexons. Bar (d and e) = 25 nm.

porated, if present. We have now analyzed the structures of such capsids, with and without VP26, in the frozen hydrated state. Our goals were to validate the baculovirus system for further, more detailed studies of capsid assembly and to effect a conclusive localization of VP26.

Recombinant baculoviruses expressing all six HSV-1 capsid genes (All) and expressing all except the UL35 gene (All − UL35) were expressed in Sf9 cells, and the capsids were purified by two cycles of sucrose gradient centrifugation (25). In terms of protein composition (Fig. 1), both capsid species closely resemble native B capsids (7, 16), except that, as expected, All − UL35 capsids lack VP26.

After dialysis to remove the sucrose, cryoelectron microscopy was performed (3, 4, 7). Most of the particles visualized were apparently intact and were very similar to the wild-type HSV-1 capsids observed in the same way (compare the capsids in Fig. 2a and c with those in references 3 and 16). However, a significant fraction had evident physical lesions. Although the particles were about the same size as the closed capsids, their assembly appears not to have been successfully completed. A higher incidence of such particles was observed when UL26 or UL26.5 was omitted (Fig. 2c). Aberrant particles were previously observed in negatively stained preparations (25), but their disrupted state could have been an air drying artifact. This explanation is ruled out when such capsids are observed as frozen hydrated specimens. Thus, baculovirus-based HSV-1 capsid assembly, while largely successful, may be more error prone than in a wild-type infection.

Micrographs selected for reconstruction were digitized, and the reconstructions were calculated by Fourier-Bessel synthesis (1, 4, 8, 26). Particle orientations were refined by the procedure of Cheng et al. (6). The All reconstruction included 37 particles from one micrograph and had a resolution of 2.7 nm according to the criterion of Conway et al. (7). The All − UL35 reconstruction required six micrographs to obtain an adequate distribution of particle orientations (1). These micrographs were mutually scaled by calculating six reconstructions and then their spherically averaged radial density profiles and by determining scale factors that maximized the match between these profiles. A composite reconstruction including 191 particles was then calculated to a resolution of 3.0 nm.

The All capsid shown in Fig. 3a and d is indistinguishable from the wild-type B capsid at the same resolution (7, 16, unpublished results). Its dimensions, its T=16 surface lattice, and the structures of its hexons, pentons, and triplexes all match the corresponding features of wild-type capsids. The All − UL35 capsid is portrayed in Fig. 3b and e. Its resolution is slightly lower, but the experimental conditions, including the degree of defocus and other microscopy related parameters, were closely similar in the two analyses. The spherically averaged radial density profiles of both kinds of capsids are compared in Fig. 4. Over the inner part of the capsid shell, i.e., between radii of ~45 and 57 nm, the two curves are superimposable. The only significant component of the difference profile (Fig. 4) is a positive peak centered at about 61 nm, implying that it is only on their outer surfaces that the capsids differ in structure.

A difference map is shown in Fig. 3c. Its only significant feature is hexameric rings of small subunits overlying the site of each hexon. No such features are seen at penton sites. The capsomers of both types of capsids are compared at higher magnification in Fig. 3d and e. The respective pentons are very similar, whereas All hexons—unlike All − UL35 hexons—have six little hornlike excrescences around their outer rims (28). The sixfold ring of subunits seen in the difference map (Fig. 3c) is set in the same orientation relative to the lattice lines as the corresponding ring seen in our previous comparison of guanidine HCl-extracted capsids before and after complementation with purified VP26 (4). The only (slight) difference in the current map is the suggestion that adjacent VP26 subunits may make contact with each other around the inner part of the ring. However, this feature is quite sensitive to the contouring level chosen and may be affected by lateral smearing arising from the limited resolution. We conclude that each such ring represents six subunits of VP26 (4).

In contrast, VP26 is clearly absent from the pentons (Fig. 4). This finding supports the inference of Zhou et al. (28), despite the conformational differences between the penton and hexon states of VP5 (see above). Among these conformational differences, one must now include structural changes around the hexon binding site for VP26 that make penton VP5 unreceptive to this ligand.

Our results establish that to at least 2.7-nm resolution, All

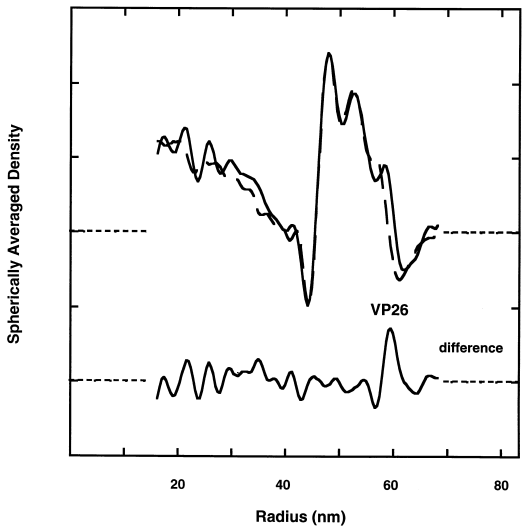

FIG. 4. (Upper part) Spherically averaged radial density profiles calculated from the three-dimensional density maps of All capsids (solid line) and All − UL35 (broken line). The two curves are superimposable between radii of ~35 nm and ~55 nm. The minima at ~45 nm and ~62 nm are artifactual, arising from phase contrast-derived interference fringes. The positive density between radii of ~15 nm and ~40 nm represents the presence of internal proteins (mainly the product of gene UL26.5). The horizontal dashed line is the solvent density baseline. Density is in arbitrary units. (Lower part) Difference between the radial density profiles. The only significant departure from zero (the baseline is the horizontal dashed line) is the peak centered at a radius of ~61 nm, which marks the location of VP26. This peak is somewhat smeared radially as a result of averaging over the various icosahedral lattice sites which lie at different radii.

capsids are structurally authentic, substantiating earlier evidence that the set of HSV-1 genes used is assembly competent (23, 25). We may conclude that any involvement of host factors (e.g., chaperonins) is confined to activities that are common to mammalian cells and insect Sf9 cells. It is possible that wild-type capsids also contain one or more minor proteins coded for by genes that were not represented in the baculovirus systems that we used. Any such proteins are evidently dispensable for morphogenesis but might have roles in subsequent events. For instance, the UL6 gene product has been reported to be a minor capsid protein required for DNA packaging (18). Moreover, it has been conjectured on the basis of similarities with capsid assembly of double-stranded DNA bacteriophages (2, 3, 5, 10) that herpesviruses may have a connector or portal protein via which DNA is packaged (22). This protein would be expected to occupy a unique vertex, distinct from the other 11. After icosahedral averaging, this vertex would contribute with a weighting of only one-twelfth to the net penton structure visualized. As a consequence, this penton would be unlikely to be visibly different from the All penton, which is an average over 12 VP5 pentamers.

The present study validates the baculovirus expression system as a flexible in vivo arena for the systematic study of HSV-1 capsid assembly. It remains to be seen what genes must be added or other modifications made to produce capsids that are competent to be packaged with DNA and to mature into infectious virions. In addition to the prospects that they offer for study of later steps of intracellular HSV capsid assembly, baculovirus expression vectors also offer a copious source of capsid proteins for in vitro assembly experiments (15). Further studies of this kind are in progress.

We thank J. Conway (NIAMS) for helpful discussions, T. Baker (Purdue University) for reconstruction software, and C. Johnson and R. Martino for making available the Intel 860 computer.

This work was supported in part by National Science Foundation grant MCB-9119056 (to J.C.B.).

REFERENCES

1. **Baker, T. S., J. Drak, and M. Bina.** 1989. The capsid of small papovaviruses contains 72 pentameric capsomeres: direct evidence from cryo-electron-microscopy of simian virus 40. Biophys. J. **55:**243–253.
2. **Baker, T. S., W. W. Newcomb, F. P. Booy, J. C. Brown, and A. C. Steven.** 1990. Three-dimensional structures of maturable and abortive capsids of equine herpesvirus 1 from cryoelectron microscopy. J. Virol. **64:**563–573.
3. **Booy, F. P., W. W. Newcomb, B. L. Trus, J. C. Brown, T. S. Baker, and A. C. Steven.** 1991. Liquid-crystalline, phage-like, packing of encapsidated DNA in herpes simplex virus. Cell **64:**1007–1015.
4. **Booy, F. P., B. L. Trus, W. W. Newcomb, J. C. Brown, J. F. Conway, and A. C. Steven.** 1994. Finding a needle in a haystack: detection of a small protein (the 12 kDa VP26) in a large complex (the 200 MDa capsid of herpes simplex virus). Proc. Natl. Acad. Sci. USA **91:**5652–5656.
5. **Casjens, S., and J. King.** 1975. Virus assembly. Annu. Rev. Biochem. **44:** 555–611.
6. **Cheng, R. H., V. Reddy, N. H. Olson, A. Fisher, T. S. Baker, and J. E. Johnson.** 1994. Functional implications of quasi-equivalence in a T=3 icosahedral animal virus established by cryo-electron microscopy and X-ray crystallography. Structure **2:**271–282.
7. **Conway, J. F., B. L. Trus, F. P. Booy, W. W. Newcomb, J. C. Brown, and A. C. Steven.** 1993. The effects of radiation damage on the structure of frozen hydrated HSV-1 capsids. J. Struct. Biol. **111:**222–233.
8. **Crowther, R. A.** 1971. Procedures for three-dimensional reconstruction of spherical viruses by Fourier synthesis from electron micrographs. Philos. Trans. R. Soc. Lond. Ser. B **261:**221–230.
9. **Davison, M. D., F. J. Rixon, and A. J. Davison.** 1992. Identification of genes encoding two capsid proteins (VP24 and VP26) of herpes simplex virus type 1. J. Gen. Virol. **73:**2709–2713.
10. **Friedmann, A., J. E. Coward, H. S. Rosenkranz, and C. Morgan.** 1975. Electron microscopic studies on assembly of herpes simplex virus upon removal of hydroxyurea block. J. Gen. Virol. **26:**171–181.
11. **Furlong, D.** 1978. Direct evidence for 6-fold symmetry of the herpesvirus hexon capsomere. Proc. Natl. Acad. Sci. USA **75:**2764–2766.
12. **Johnson, C. A., N. I. Weisenfeld, B. L. Trus, J. F. Conway, R. L. Martino, and A. C. Steven.** 1994. Orientation determination in the 3D reconstruction of icosahedral viruses using a parallel computer, p. 550–559. *In* Proceedings of Supercomputing 94. IEEE Computer Society, Los Alamitos, Calif.
13. **McNabb, D. S., and R. J. Courtney.** 1992. Identification and characterization of the herpes simplex virus type 1 virion protein encoded by the UL35 open reading frame. J. Virol. **66:**2653–2663.
14. **Newcomb, W. W., J. C. Brown, F. P. Booy, and A. C. Steven.** 1989. Nucleocapsid mass and capsomer protein stoichiometry in equine herpesvirus 1: scanning transmission electron microscopic study. J. Virol. **63:**3777–3783.
15. **Newcomb, W. W., F. L. Homa, D. R. Thomsen, Z. Ye, and J. C. Brown.** 1994. Cell-free assembly of the herpes simplex virus capsid. J. Virol. **68:**6059–6063.
16. **Newcomb, W. W., B. L. Trus, F. P. Booy, A. C. Steven, J. S. Wall, and J. C. Brown.** 1993. Structure of the herpes simplex virus capsid: molecular composition of the pentons and triplexes. J. Mol. Biol. **232:**499–511.
17. **Palmer, E. L., M. L. Martin, and G. W. Gary, Jr.** 1975. The ultrastructure of disrupted herpesvirus nucleocapsids. Virology **65:**260–265.
18. **Patel, A. H., and J. B. MacLean.** 1995. The product of the UL6 gene of herpes simplex virus type 1 is associated with virus capsids. Virology **206:** 465–478.
19. **Rixon, F. J.** 1993. Structure and assembly of herpesviruses. Semin. Virol. **4:**135–144.
20. **Schrag, J. D., B. V. Prasad, F. J. Rixon, and W. Chiu.** 1989. Three-dimensional structure of the HSV1 nucleocapsid. Cell **56:**651–660.
21. **Steven, A. C., C. R. Roberts, J. Hay, M. E. Bisher, T. Pun, and B. L. Trus.** 1986. Hexavalent capsomers of herpes simplex virus type 2: symmetry, shape, dimensions, and oligomeric status. J. Virol. **57:**578–584.
22. **Steven, A. C., and P. G. Spear.** Herpesvirus capsid assembly and envelopment. *In* W. Chiu, R. Burnett, and R. Garcea (ed.), Structural biology of viruses, in press. Oxford University Press, Oxford.
23. **Tatman, J. D., V. G. Preston, P. Nicholson, R. M. Elliott, and F. J. Rixon.** 1994. Assembly of herpes simplex virus type 1 capsids using a panel of recombinant baculoviruses. J. Gen. Virol. **75:**1101–1113.
24. **Thomsen, D. R., W. W. Newcomb, J. C. Brown, and F. L. Homa.** 1995. Assembly of the herpes simplex virus capsid: requirement for the carboxyl-terminal twenty-five amino acids of the proteins encoded by the UL26 and UL26.5 genes. J. Virol. **69:**3690–3703.
25. **Thomsen, D. R., L. L. Roof, and F. L. Homa.** 1994. Assembly of herpes simplex virus (HSV) intermediate capsids in insect cells infected with recombinant baculoviruses expressing HSV capsid proteins. J. Virol. **68:**2442–2457.
26. **Trus, B. L., W. W. Newcomb, F. P. Booy, J. C. Brown, and A. C. Steven.** 1992. Distinct monoclonal antibodies separately label the hexons or the pentons of herpes simplex virus capsid. Proc. Natl. Acad. Sci. USA **89:**11508–11512.
27. **Wildy, R., W. C. Russell, and R. W. Horne.** 1960. The morphology of herpes virus. Virology **12:**204–222.
28. **Zhou, Z. H., B. V. V. Prasad, J. Jakana, F. J. Rixon, and W. Chiu.** 1994. Protein subunit structures in the herpes simplex virus capsid determined from 400-kV spot-scan electron cryomicroscopy. J. Mol. Biol. **242:**456–469.